King Saud University

Arabian Journal of Chemistry

www.ksu.edu.sa
www.sciencedirect.com

ORIGINAL ARTICLE

Citrus sinensis leaf aqueous extract green-synthesized silver nanoparticles: Characterization and cytotoxicity, antioxidant, and anti-human lung carcinoma effects

Fangshan Chen [a,1], Qing Zheng [b,1], Xiaoting Li [c], Jie Xiong [d,*]

[a] *Department of Oncology and Hematology, The Affiliated Traditional Chinese Medicine Hospital of Southwest Medical University, Luzhou, Sichuan 646000, China*
[b] *Department of Clinical Laboratory, Haikou Hospital Of Maternal And Child Health· Haikou Women&Children Hospital, Haikou, Hainan 570102, China*
[c] *Zhengzhou University of Industrial Technology, Zhengzhou, Henan 451150, China*
[d] *Cancer Center, Union Hospital, Tongji Medical College, Huazhong University of Science and Technology, Wuhan, Hubei 430022, China*

Abstract The present work demonstrates the synthesis of Ag nanoparticles (Ag NPs) by using aqueous extract of *Citrus sinensis* as green reductant and capping agent without any toxic reagent. Physicochemical characteristics of the said nanoparticles were elucidated by **field emission scanning electron microscopy (FESEM), fourier transform infrared spectroscopy (FTIR), and ultraviolet–visible spectroscopy (UV-Vids)** techniques. The biogenic Ag NPs are uniformly globular. The Ag NPs has been explored biologically in the anticancer and antioxidant assays. In the cellular and molecular part of the recent study, the treated cells with Ag NPs were assessed by MTT assay for 48 h about the cytotoxicity and anti-human lung carcinoma properties on normal (HUVEC) and lung carcinoma cell lines i.e. NCI-H661, HLC-1, NCI-H1563, LC-2/ad, NCI-H1299, and PC-14. The viability of malignant lung cell line reduced dose-dependently in the presence of Ag NPs. The IC50 of Ag NPs were 82, 139, 170, 66, 62, and 50 μg/mL against NCI-H661, HLC-1, NCI-H1563, LC-2/ad, NCI-H1299, and PC-14 cell lines, respectively. In the antioxidant test, the IC50 of Ag NPs and vitamin E against **2,2-diphenyl-1-picrylhydrazyl (DPPH)** free radicals were 21 and 15 μg/mL,

* Corresponding author.
E-mail address: xiongjie_2021@outlook.com (J. Xiong).
[1] Fangshan Chenand Qing Zheng are co-first aothors, they contributed equally to this work.

Production and hosting by Elsevier

respectively. After clinical study, Ag NPs containing *Citrus sinensis* leaf aqueous extract may be used to formulate a new chemotherapeutic drug or supplement to treat the several types of human lung adenocarcinoma.

1. Introduction

The biological distribution of therapeutic agents can be a fundamental factor in these fractures. Inadequate concentration at unwanted concentration and target sites elsewhere, leading to dose-limiting poisoning (Wolach and Blood, 2015; Abdel-Fattah and Ali, 2018). The biological distribution of drug agents is controlled largely by the drugs ability to penetrate biological barriers. Strategy for Adding Targeting Sections to Therapeutic Nanoparticles to Improve Location Specification to date, despite 30 years of effort in pharmaceutical companies and many laboratories, it has not yet been able to produce clinically approved drugs (GBD, 2015; Ball, 2018). This failure is because the addition of molecular agents increases the targeting of cognitive characteristics. However, it does so in the face of much greater difficulty in managing biological barriers (Sintubin et al., 2009; Ahmed et al., 2016; Varma, 2012; Sivaraj et al., 2014; Sharma et al., 2009).

Metallic nanoparticles have gained significant attention in the area of biomedical technology. (Nadagouda and Varma, 2006; Rajeshkumar, 2016; Raut et al., 2010) It has been revealed that metallic nanoparticles synthesized using plants have excellent noncytotoxicity potential against human normal cells, antioxidant property against free radicals such as DPPH, antibacterial activities against Gram positive and negative bacteria and antifungal activities against *Candida* species. (Zangeneh, 2019) There are many methods for producing metallic nanoparticles including; a) Physical method, b) Chemical method, c) Biological method. (Ahmed et al., 2016; Varma, 2012; Sivaraj et al., 2014) In biological nanoparticle synthesis, various microbes, enzymes, algae, and especially plants have been used and served as a suitable alternative method to physical and chemical procedures with high therapeutic potentials. (Sharma et al., 2009; Nadagouda and Varma, 2006; Rajeshkumar, 2016; Raut et al., 2010).

Metallic nanoparticles were used for their anticancer properties against several cell lines such as MDAMB231(human breast adenocarcinoma), human colorectal adenocarcinoma cells, MCF7 (human breast adenocarcinoma), HeLa (human cervical adenocarcinoma cells), HepG2 (human liver cancer cells), HCT-116 (colon cancer cells), SKBR3 (human breast adenocarcinoma cells), A549 (human lung carcinoma cells), and human chronic myelogenous cells. (GBD, 2015).

In the previous study, Klein et al. (Klein et al., 2014) indicated that metallic nanoparticles with range sizes of 9–20 nm could treat the breast and colon cancers. They investigated the Caco-2 and MCF-7 cell lines for analyzing the anti-breast and anti-colon cancer properties of iron nanoparticles, respectively. (Klein et al., 2014) Also, in the study of Namvar et al. (Namvar et al., 2014) has been indicated that metallic nanoparticles synthesized using plant extracts have excellent cytotoxicity potentials against Jurkat cells (Human cell lines for leukemia), MCF-7 cells (breast cancer), HeLa cells (cervical cancer), and HepG2 cells (liver cancer). (Namvar et al., 2014).

In the previous study indicated that ethno medicinal plants have a suitable ability in the treatment of cancer. A list of medicinal plants that have been used for increasing the anti-cancer activities includes *Maytenus boaria*, *Cephaelis acuminate*, *Barleria prionitis*, *Boswellia serrate*, *Lavendula officinalis*, *Cephalotaxus harringtonia* drupacea, *Tinospora cordifolia*, *Euphoria hirta*, *Lubinus perennis*, *Sophora subprostrata*, *Phyllanthus niruri*, and *Solanum seaforthianum*. (Soni and Krishnamurthy, 2013).

Accordingly, the current study was conducted to evaluate the possible protective activity of synthesized silver nanoparticles using *Citrus sinensis* leaf aqueous extract against common cell lines of lung cancer in the in vitro condition.

2. Experimental

2.1. Material

All materials were obtained from Sigma Aldrich chemicals.

2.2. Preparation and extraction of Citrus sinensis leaf

Collected fresh leaf of *Citrus sinensis* were shade-dried at room temperature for 21 days. The dried leaf were then milled into fine powder by use of an electric mill. The powdered plant material was kept at room temperature away from direct sunlight in a dry airtight plastic container ready for extraction. For extraction, five hundred grams of the powdered *Citrus sinensis* leaf were soaked in 5 L of distilled water and swirled regularly for 24hrs. The extract was decanted, filtered using muslin cloth into a different dry clean conical flask. The filtrate was concentrated under reduced pressure using a rotary evaporator at 40◦C to obtain a semi-solid residue. (Tahvilian et al., 2019).

2.3. Preparation and synthesis of Ag NPs

The green synthesis of the silver nanoparticles was initiated with a reaction mixture of 100 mL of silver salt (AgNO$_3$) in the concentration of 1×10^{-3} M and 200 mL of aqueous extract solution of plant leaf (20 µg/mL) in the proportion 1:10 in a conical flask.

The reaction mixture was kept under magnetic stirring for 12 h at room temperature. At the end of the reaction time, the black colored colloidal solution of Ag was formed. The mixture was centrifuged at 10000 rpm for 15 min. The precipitate was triplet washed with water and centrifuged subsequently (Mohammadi et al., 2019).

2.4. Chemical characterization

In this research, to record the UV–vis spectra, a Shimadzu UV spectrophotometer was used. Also, JASCO (FT/IR-6200) spectrophotometer was utilized to record the FT-IR spectra in this research. To evaluate the different morphological characteristic of nanoparticles such as size distribution, surface morphology and the particle shape, MIRA3TESCAN-XMU FE-SEM was used to record Field Emission Scanning Electron Microscopy (FE-SEM) images.

2.5. Analysis of antioxidant properties

In this method, 1 mL of different concentrations of the nanoparticles (0–1000 μg/ml) (with 1 mL of DPPH (300 μmol/l) combined and then the final volume of the combination with methanol reached 4000 μL. The falcons were then vertexed and kept in the dark for 60 min. The absorbance was read at 517 nm. The DPPH radical inhibition percentage was calculated using the following equation (Tahvilian et al., 2019):

$$\text{Inhibition}(\%) = \frac{\text{Sample A.}}{\text{Control A.}} \times 100$$

In this formula:

Sample A is the rate of sample absorption, control A is the rate of control absorption at 517 nm.

2.6. Analysis of cell toxicity

In this experiment, NCI-H661, HLC-1, NCI-H1563, LC-2/ad, NCI-H1299, and PC-14 (Lung carcinoma cell lines) and HUVEC (Human umbilical vein endothelial cells: Normal cell line) were provided from Pasteur Institute of Iran for investing the cytotoxicity properties of the nanoparticles using an MTT assay. These cells were cultured in Dulbecco's modified Eagle's medium (DMEM) with 10% (w/v) FBS, 100U/mL penicillin, and 100 μg/mL streptomycin. Then, cells were distributed at 10,000 cells/well in 96-well plates. The cells were grown under a humidified incubator with 5% CO_2 at 37 °C until reaching confluency (typically after 24 h). The cells were treated with nanoparticles at concentrations of 0, 1, 2, 3, 7, 15, 31, 62, 125, 250, 500, and 1000 μg/mL and subsequently incubated for 2 and 24 h. Nanoparticles were sterilized using UV radiation for 1 h. Finally, the MTT solution (5 mg/mL in PBS) was added to each well and incubated for 4 h at 37 °C. The medium with MTT was removed and the formazan crystals formed in the living cells were dissolved in 100 μL Dimethyl sulfoxide (DMSO) per well. All tests were run in the triplicates. The relative viability (%) was calculated based on the absorbance at λ = 570 nm determined using a microplate reader: (Mohammadi et al., 2019).

$$\text{Cell viability } (\%) = \frac{\text{Sample A.}}{\text{Control A.}} \times 100$$

2.7. Data management and statistical analysis

The data on absorbance measures were entered in the Microsoft® Excel spreadsheet one-word program, where it was organized and then exported to Minitab statistical software for analysis. This was found to conform with assumptions of parametric data and expressed as Means ± Standard Deviations (SD). All statistical analyses were performed using Minitab (Minitab 17.1 Version, NC, USA). The analyzed data was presented in Figures.

3. Results and discussion

3.1. Chemical characterization

The FE-SEM device is one of the most powerful tools used in various fields, including nanotechnology, which uses electron bombardment to produce images of objects as small as 10 nm. The bombardment of the sample causes positively charged electrons to be released from the sample to the plate, where these electrons become signals. (Mohammadi et al., 2019).

The surface morphology and size of Ag NPs were investigated using field emission scanning electron microscope (FE-SEM). The Fig. 1 depicts a successful synthesis of silver nanoparticles with spherical morphology that was reported previously. (Mohammadi et al., 2019) The pictures also approve uniformity, well dispersed and homogeneous of the biosynthesized Ag NPs. A tendency for aggregation for the synthetic nanoparticles as well as is observed. This property of metallic nanoparticles such as Ag NPs, CdNPs, CuNPs, AgNPs, and TiNPs that were synthesized using environmentally friendly methods has been previously reported. (Tahvilian et al., 2019201920192019; Mohammadi et al., 2019). The diameter of particle size for Ag NPs was on average of 78.12 nm.

FT-IR (Fourier Transform Infrared) has been a suitable technique for analyzing materials in the laboratory. An infrared spectrum represents the fingerprint of the sample under test with absorption peaks, which depends on our vibrational frequencies between the atomic bonds of that material. Since each substance has its own atomic bonds, no two compounds with the same infrared spectrum are alike. Hence, infrared spectroscopy can be effective in better identification (qualitative analysis) of different types of materials. In addition, the peak sizes are in the range indicating the amount of material present. Advanced software algorithms make this spectroscopy a great tool for quantitative analysis (Tahvilian et al., 2019; Mohammadi et al., 2019).

In FT-IR spectra, the peaks in the region between 400 and 700 cm-1 are attributed to metal–oxygen vibration. In this study (Fig. 2), the formation of silver nanoparticles can be confirmed by the presence of a peak at 496 and 541 cm-1 belong to bending vibration of Ag―O. The appearance of these peaks, with a small difference in the wavenumber, have been reported previously for biosynthetic Ag NPs. (Vivek et al., 2012; Justin Packia Jacob et al., 2012; Matthäus, 2020) The presences of secondary metabolites, which are responsible for the capping and reduction of Ferric chloride precursor to Ag NPs, has been studied using FT-IR technique. The presences of different-IR bands related to existences of various functional groups in Citrus sinensis extract. In this study, the IR spectra investigated for the silver nanoparticles revealed the absorption peaks at (I) 2871 and 3339 cm-1 (OH group of alcohols and phenols); (II) 1614 cm-1 (C―O group of carboxylic acid group); (III) 1418 cm-1 (C=O stretching of carboxylic acid group); (IV) 1007 and 1269 cm-1 (C―OH vibrations of the protein/polysaccharide). The above peaks were confirmed in the previous studies. (Ishino et al., 2020; Beheshtkhoo et al., 2018; Oganesvan et al., 1991) According to Ghidan et al. (2016) report, the plant extracts were bounded to metallic nanoparticles through hydroxyl and carbonyl of biomolecules as reducing, stabilizing, and dispersing agents (Oganesvan et al., 1991) Fig. 3.

UV–Vis is based on the irradiation of ultraviolet and visible photons on the sample and measures the rate of passage or absorption of matter at different wavelengths in the range of 200 to 1100 nm. It is possible to measure the spectrum for samples in solution, solid as well as thin layers. The size of solid
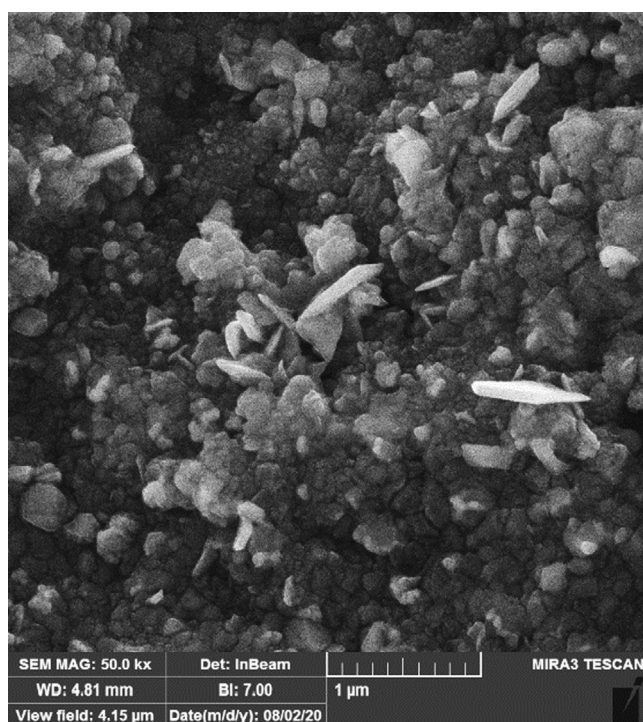
Fig. 1 FE-SEM image of Ag NPs.

samples should be larger than 20 mm. This test is not possible for powder samples. One of the important applications of UV device is to determine the concentration of the unknown solution. By having the original sample and its solvent and making several solutions with different percentages and drawing a calibration diagram based on the calculation of the maximum land, the concentration of the unknown solutions can be calculated. (Arulmozhi et al., 2013; You et al., 2012).
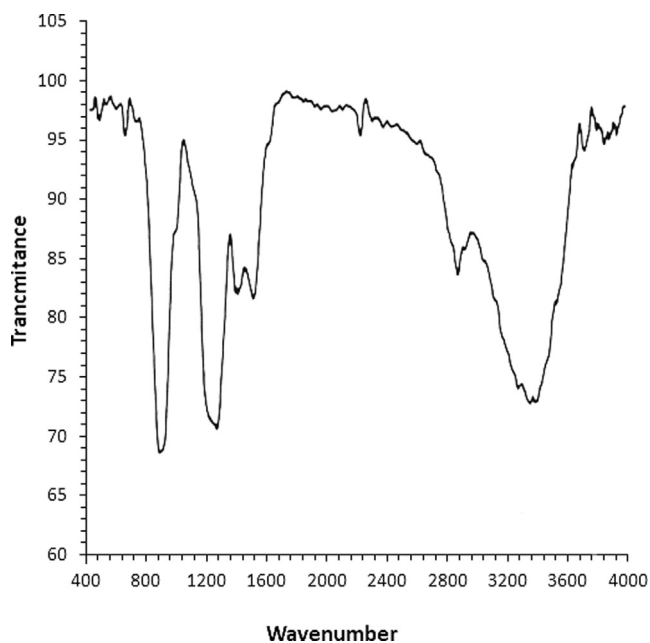
Fig. 2 FT-IR analysis of Ag NPs.
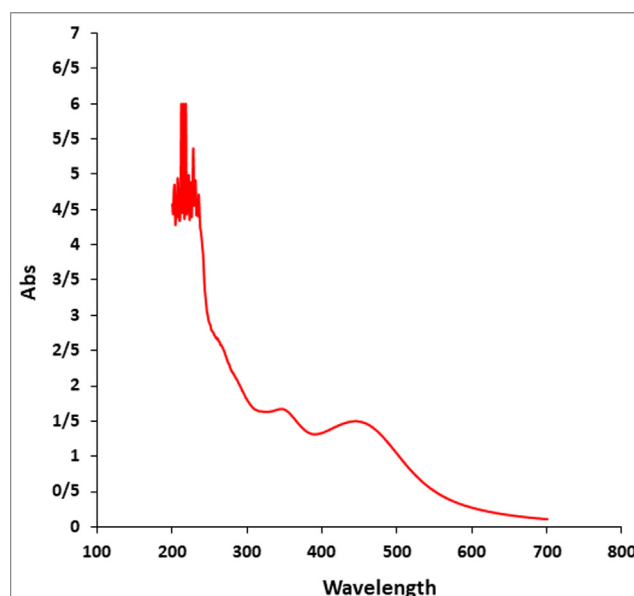
Fig. 3 UV–VIs analysis of Ag NPs.

The UV–Vis. spectra of biosynthesized Ag NPs using the aqueous extract of *Citrus sinensis* is shown in Fig. 1. The optical properties, which obtained from the UV–Vis. spectroscopy result, confirmed the formation of Ag NPs. One peak at 446 nm belongs to the synthetic Ag NPs. This observation is in good agreement to the previous studies on biosynthesized of Ag NPs. (Arulmozhi et al., 2013; You et al., 2012).

3.2. Antioxidant analysis

Traditional medicinal plants are well-known and essential natural antioxidant sources. Medicinal plant-derived natural antioxidants, which are in the form of raw extracts and/or chemical constituents, are very efficient in blocking the process of oxidation by neutralizing free radicals. It is also commonly accepted that medicines taken from plant products are safer than their synthetic counterparts; however, the toxicity profile of most medicinal plants have not been comprehensively assessed (Oganesvan et al., 1991; Arulmozhi et al., 2013; You et al., 2012). Combining them with metallic salts is a good option for increasing the antioxidant competencies of therapeutic plants. In previous studies, a significant increase in antioxidant properties has been reported when produced by green synthesis with salts such as gold, silver, copper and iron (Mohammadi et al., 2019). In the study, concentration-dependent DPPH radical scavenging effect of *Citrus sinensis* leaf extract and AgNPs such as vitamin E was observed. The interaction between *Citrus sinensis* leaf aqueous extract and AgNPs and DPPH may have occurred by transferring electrons and hydrogen ions to the "2,2-diphenyl-1-picrylhydrazy l" radical to form a stable "2,2-diphenhydrazine"."Molecule (DPPH) (Tahvilian et al., 2019; Mohammadi et al., 2019). The IC50 values of vitamin E and AgNPs were 15 and 21 µg/mL, respectively (Fig. 4 and Table 1). The antioxidant property created by *Citrus sinensis*, which is caused by the presence of various phytochemicals, may be thought to be neutralizer for reactive nitrogen species (RNS) and reactive oxygen species (ROS) (Vivek et al., 2012).
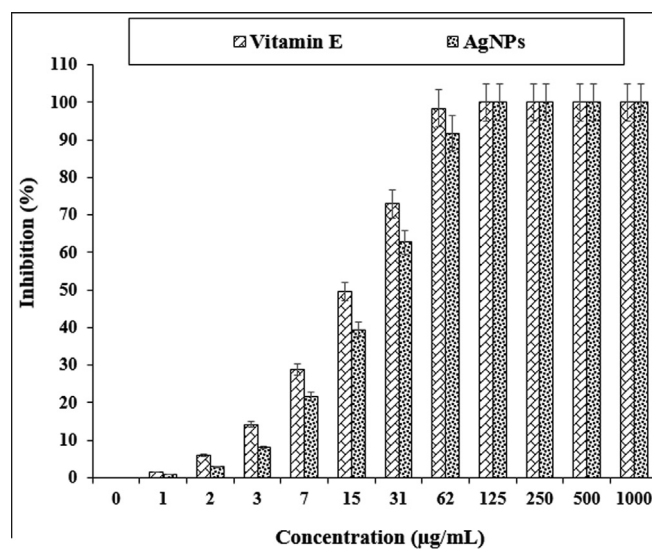
Fig. 4   The antioxidant properties of AgNPs and vitamin E.

Table 1   The IC50 of AgNPs and vitamin E in the antioxidant test.

	AgNPs	Vitamin E
IC50 (μg/mL)	21 ± 0^a	15 ± 0^a

3.3. Cytotoxicity and anti-lung cancer effects

Nanotechnology is a new branch of science with a wide range of applications and nanoparticles with different compositions and sizes, shapes and surface chemical properties can have different biological and biomedical applications. Reducing the size of materials at the nanoscale can often cause electrical, magnetic, structural, morphological, and chemical changes. Nanoparticles typically have a higher percentage of atoms on their surface, which increases surface reactions. (Nadagouda and Varma, 2006; Rajeshkumar, 2016; Raut et al., 2010; Zangeneh, 2019) Proper design of nanomaterials can be used to target specific cancer cells. Nanoparticles have antibacterial and magnetic properties by penetrating microorganisms due to their high surface-to-volume ratio and small size. Also, due to their photocatalytic, catalytic and ionic properties, they are widely used in the fight against human pathogenic microbes, bacteria, fungi and viruses. (Tahvilian et al., 2019; Mohammadi et al., 2019) Researchers have shown that silver nanoparticles kill Schwann cells by releasing Ag +. A study has shown that concomitant use of silver and doxorubicin reduces the reproductive toxicity of doxorubicin. (Namvar et al., 2014; Justin Packia Jacob et al., 2012) By producing active bases such as oxygen ions and hydroxides, silver nanoparticles disrupt the metabolism, proliferation and respiration of microorganisms by destroying organic structures
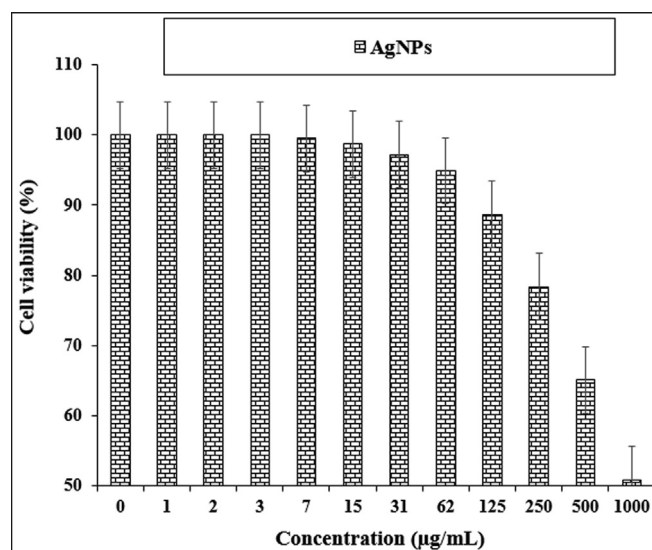
Fig. 5   The cytotoxicity properties of AgNPs against normal cell line.
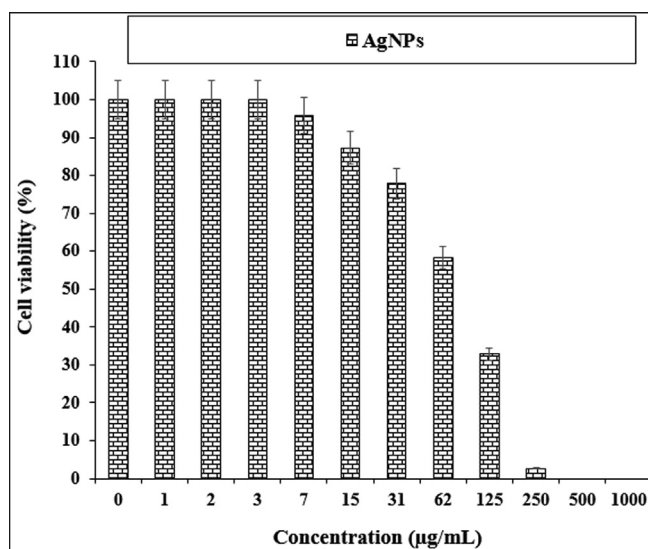
Fig. 6   The anti-human lung cancer properties of AgNPs against NCI-H661 cell line.

and strongly interacting with enzymes and proteins in the electron transfer system, and it can kill more than 650 types of gram-negative and gram-positive bacteria resistant to common antibiotics in vitro up to 99.9%. (Namvar et al., 2014) Metallic nanoparticles in cell cultures and human tissues yield toxins that raise inflammatory products such as cytokines and oxidative stress, ultimately leading to cell death. Larger nanoparticles are seen by the nuclei and mitochondria, causing mutations in DNA, destruction of the mitochondrial structure, and even cell death. (Sivaraj et al., 2014; Sharma et al., 2009; Nadagouda and Varma, 2006) Solubility and density, surface baroelectricity, surface structure, shape, chemical composition, and size and dimensions are the key factors in determining the toxicity of nanoparticles. The exact effect of silver and silver nanoparticles on cancer cells is not fully understood, but increasing ROS production is one of the possible mechanisms. (Namvar et al., 2014; Justin Packia Jacob et al., 2012) When

nanoparticles are in contact with cancer cells, the cellular defense mechanism is activated to minimize damage. But, if the ROS production stimulation inside the cell by nanoparticles exceeds the cell antioxidant defense capacity, the cells are destroyed during the process of apoptotic cell death. (Raut et al., 2010; Zangeneh, 2019; Klein et al., 2014; Namvar et al., 2014; Soni and Krishnamurthy, 2013; Tahvilian et al., 2019) The electrostatic interaction of nanoparticles causes them to be absorbed into target cells. Positively charged nanoparticles are attracted to cancer cells with a high percentage of anionic phospholipids and certain groups of charged proteins and carbohydrates on their outer surface. (Tahvilian et al., 2019; Mohammadi et al., 2019).

The treated cells with various concentrations of the present $AgNO_3$, Citrus sinensis leaf aqueous extract, and silver nanoparticles were examined by MTT test for 48 h regarding the cytotoxicity and anti-human lung cancer potentials on nor-
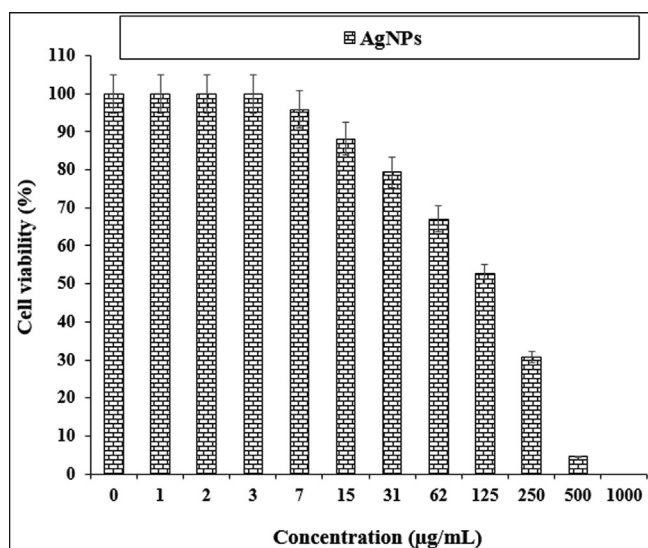
Fig. 7   The anti-human lung cancer properties of AgNPs against HLC-1 cell line.
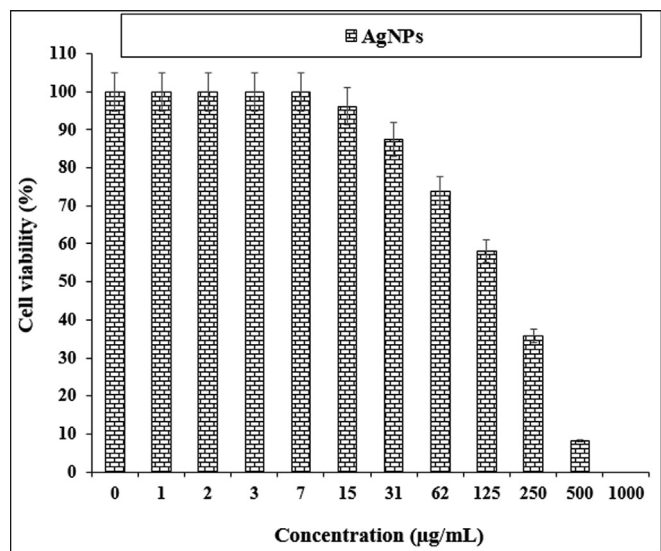
Fig. 8   The anti-human lung cancer properties of AgNPs against NCI-H1563 cell line.

mal (HUVEC) and common human lung cancer (NCI-H661, HLC-1, NCI-H1563, LC-2/ad, NCI-H1299, and PC-14) cell lines (Figs. 5-11; Table 2). The absorbance rate for AgNO$_3$, *Citrus sinensis* leaf aqueous extract and silver nanoparticles was measured at 570 nm, showing exceptional viability in the normal cell line (HUVEC) up to 1000 μg/mL.

The viability of specific lines of human lung cancer cells decreased dose-dependently in the presence of AgNO$_3$, *Citrus sinensis* leaf aqueous extract, and silver nanoparticles.

The results of many studies have revealed that AgNPs released by AgNPs and Ag are involved in the anticancer mechanism in several ways: AgNPs are likely to have an excellent surface outside of the mitochondria to selectively remove oxygen from superoxide in the electron-to-electron transport chain. (Matthäus, 2020; Ishino et al., 2020; Beheshtkhoo et al., 2018).

1) Ag interferes with its functions by binding to proteins and DNA (Beheshtkhoo et al., 2018).

Silver nanoparticles' anticancer is largely dependent on a variety of factors relating to their physical properties, such as surface coating, shape and thickness.

Around the size, it has been documented that small-sized silver nanoparticles can migrate and extract tumor cells from the cell membrane. On a larger scale, the above capability is significantly limited (Oganesvan et al., 1991). As can be seen in Fig. 1 of our study, silver nanoparticles had a homogeneous spherical morphology in an average range of 78.12 nm. The size of silver nanoparticles below 50 nm is well suited for killing tumor cell lines (Oganesvan et al., 1991).

Likely, the significant anti-human lung cancer potentials of silver nanoparticles synthesized by plant leaf aqueous extract
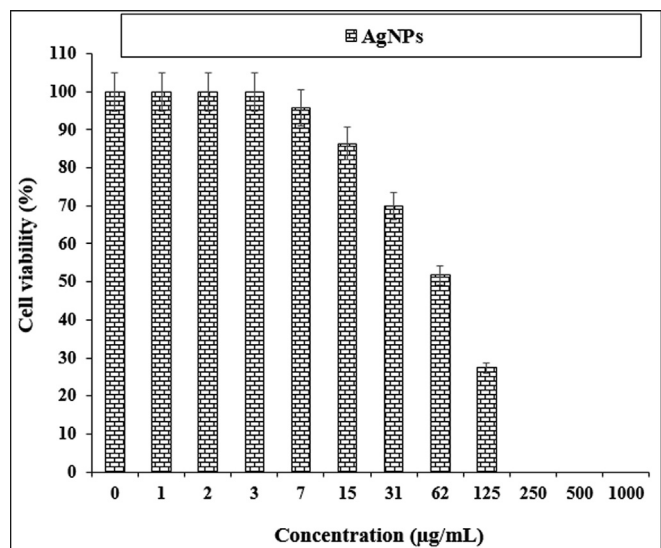
Fig. 9   The anti-human lung cancer properties of AgNPs against LC-2/ad cell line.
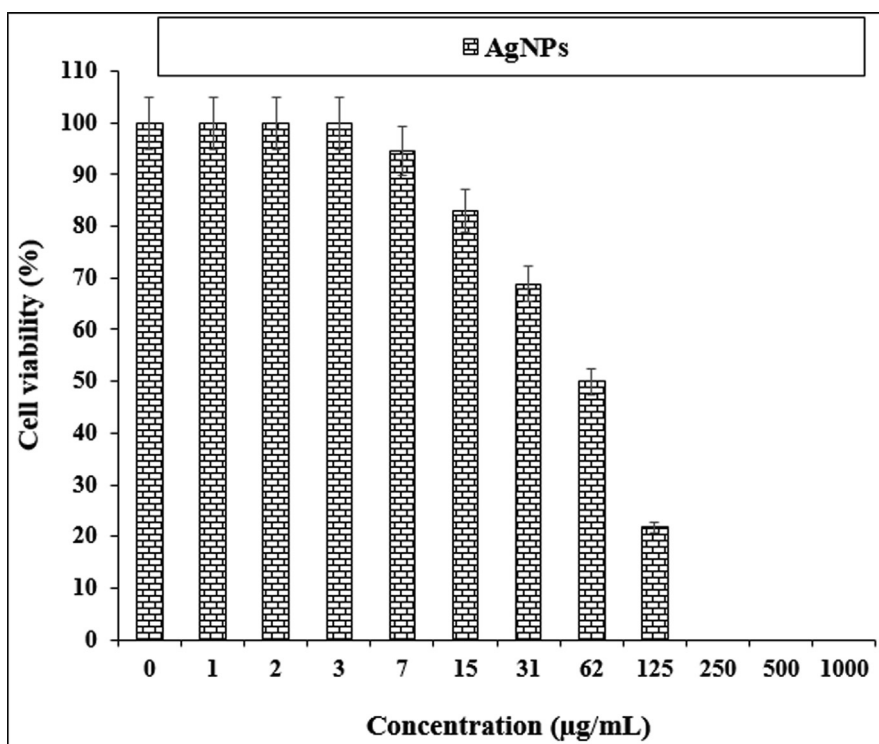
Fig. 10   The anti-human lung cancer properties of AgNPs against NCI-H1299 cell line.
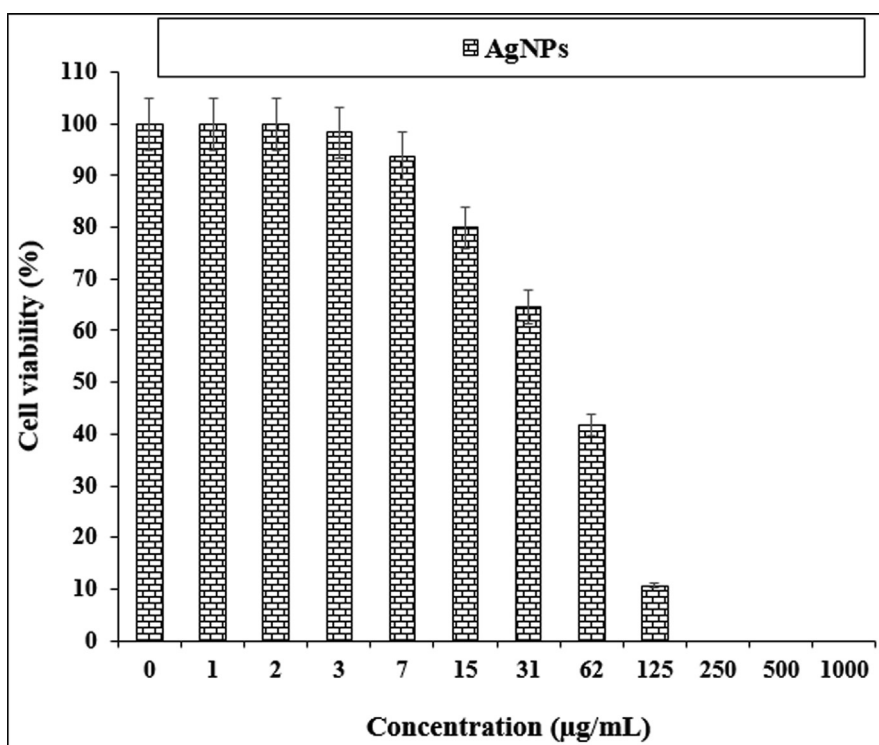
Fig. 11   The anti-human lung cancer properties of AgNPs against PC-14 cell line.

against common human lung cancer cell lines are linked to their antioxidant activities. Similar researches have revealed the antioxidant materials such as metallic nanoparticles especially silver nanoparticles and ethnomedicinal plants reduce

the volume of tumors by removing free radicals (Radini et al., 2018; Sankar et al., 2014). In detail, the high presence of free radicals in the normal cells makes many mutations in their DNA and RNA, destroys their gene expression and then

Table 2 The IC50 of AgNPs in the anti-human lung cancer test.

	HUVEC	NCI-H661	HLC-1	NCI-H1563	LC-2/ad	NCI-H1299	PC-14
IC50 (μg/mL)	–	82 ± 0^a	139 ± 0^b	170 ± 0^b	66 ± 0^a	62 ± 0^a	50 ± 0^a

accelerates the proliferation and growth of abnormal cells or cancerous cells[38–40]. The free radicals high presences in all cancers such as breast, gallbladder, stomach, rectal, liver, gastrointestinal stromal, esophageal, bile duct, small intestine, pancreatic, colon, parathyroid, thyroid, bladder, prostate, testicular, fallopian tube, vaginal, lung, hypopharyngeal, throat, lung, and skin cancers indicate a significant role of these molecules in making angiogenesis and tumorigenesis (Sankar et al., 2014; Sangami and Manu, 2017). Many researchers reported that silver nanoparticles synthesized by ethnomedicinal plants have a remarkable role in removing free radicals and growth inhibition of all cancerous cells (Namvar et al., 2014; Katata-Seru et al., 2018).

4. Conclusion

*s*Ps as a suitable and safe material. After AgNPs synthesizing, they characterized and analyzed by FT-IR, UV–Vis., and FE-SEM. The above tests indicated that these nanoparticles were synthesized as the best possible form. In the FE-SEM image, AgNPs were spherical with an average size of 78.12 nm. In UV– Vis, the clear peak in the wavelength of 446 nm indicated the formation of AgNPs. In addition, in the FT-IR test, the presence of many antioxidant compounds with related bonds caused excellent conditions for reducing silver in the AgNPs. In the biological experiments, AgNPs revealed excellent antioxidant and anti-human lung cancer effects. It seems theses nanoparticles may be used in medicine as a chemotherapeutic supplement or drug.

References

Wolach, O., Blood, R.M., 2015. 125, 2477–2485.

Abdel-Fattah, W.I., Ali, G.W., 2018. J. Appl. Biotechnol. Bioeng. 5, 00116.

GBD, 2015 Disease and Injury Incidence and Prevalence, Collaborators. "Global, regional, and national incidence, prevalence, and years lived with disability for 310 diseases and injuries, 1990-2015: a systematic analysis for the Global Burden of Disease Study 2015". *Lancet*. 2016, *388*, 1545–1602.

Ball, V., 2018. Front. Bioeng. Biotechnol. 17, 109.

Sintubin, L., Windt, W.D., Dick, J., Mast, J., van der Ha, D., Verstraete, W., 2009. Appl. Microbiol. Biotechnol. 84, 741–749.

Ahmed, S., Ahmad, M., LalSwami, B., Ikram, S., 2016. J. Adv. Res. 7, 17–28.

Varma, R.S., 2012. Curr. Opin. Chem. Eng. 1, 123.

Sivaraj, R., Pattanathu, K., Rajiv, P., Hasna, S., Venckatesh, R., 2014. Acta Part A: Mol. Biomol. Spectrosc. 133, 178–181.

Sharma, V.K., Yngard, R.A., Lin, Y., 2009. Adv. Colloid Interface Sci. 145, 83.

Nadagouda, M.N., Varma, R.S., 2006. Green Chem. 8, 516.

Rajeshkumar, S., 2016. Resour Effic Technol. 2, 230.

Raut, R.W., Kolekar, N.S., Lakkakula, J.R., Mendhulkar, V.D., Kashid, S.B., 2010. Nano-Micro Lett. 2, 106.

Zangeneh, M.M., 2019. Appl. Organometal. Chem. e4963

Klein, S., Sommer, A., Distel, L.V., Hazemann, J.L., Kröner, W., Neuhuber, W., Müller, P., Proux, O., Kryschi, C., 2014. J. Phys. Chem. B 118, 6159–6166.

Namvar, F., Rahman, H.S., Mohamad, R., Baharara, J., Mahdavi, M., Amini, E., Chartrand, M.S., Yeap, S.K., 2014. Int. J. Nanomed. 19, 2479–2488.

Soni, A., Krishnamurthy, R., 2013. Indian J. Plant Sci. 2, 117–125.

(a) Tahvilian, R., Zangeneh, M.M., Falahi, H., Sadrjavadi, K., Jalalvand, A.R., Zangeneh, A., 2019. Appl. Organometal Chem., e5234. (b) Jalalvand, A.R., Zhaleh, M., Goorani, S., Zangeneh, M. M., Seydi, N., Zangeneh, A., Moradi, R., 2019. J. Photochem. Photobiol. B. 192, 103–112. (c) Zangeneh, M.M., Zangeneh, A., Pirabbasi, E., Moradi, R., Almasi, M., 2019. Appl. Organometal. Chem., e5246. (d) Mahdavi, B., Paydarfard, S., Zangeneh, M.M., Goorani, S., Seydi, N., Zangeneh, A., 2019. Appl. Organometal Chem., e5248.

(a) Mohammadi, G., Zangeneh, M.M., Zangeneh, A., Siavash Haghighi, Z.M., 2019. Appl Organometal Chem., e5136. (b) Zangeneh, M.M., Saneei, S., Zangeneh, A., Toushmalani, R., Haddadi, A., Almasi, M., Amiri-Paryan, A., 2019. Appl Organometal Chem., e5216. (c) Zangeneh, M.M., Joshani, Z., Zangeneh, A., Miri, E., 2019. Appl Organometal Chem e5016. (d) Zangeneh, A., Zangeneh, M.M., Moradi, R., 2019. Appl. Organometal Chem. e5247.

Vivek, R., Thangam, R., Muthuchelian, K., et al, 2012. Green biosynthesis of silver nanoparticles from Annona squamosa leaf extract and its in vitro cytotoxic effect on MCF-7 cells. Process Biochem. 47, 2405–2410. https://doi.org/10.1016/j.procbio.2012.09.025.

Justin Packia Jacob, S., Finub, J.S., Narayanan, A., 2012. Synthesis of silver nanoparticles using Piper longum leaf extracts and its cytotoxic activity against Hep-2 cell line. Colloids Surf. B Biointerfaces 91, 212–214. https://doi.org/10.1016/j.colsurfb.2011.11.001.

Matthäus, B., 2020. Antioxidant activity of extracts obtained from residues of different oilseeds. J. Agric. Food Chem. 50, 3444–3452. https://doi.org/10.1021/jf011440s.

Ishino, K., Wakita, C., Shibata, T., et al, 2020. Lipid peroxidation generates body odor component trans-2-nonenal covalently bound to protein in vivo. J. Biol. Chem. 285, 15302–15313. https://doi.org/10.1074/jbc.M109.068023.

Beheshtkhoo, N., Kouhbanani, M.A.J., Savardashtaki, A., et al, 2018. Green synthesis of iron oxide nanoparticles by aqueous leaf extract of Daphne mezereum as a novel dye removing material. Appl. Phys. A 124, 363–369. https://doi.org/10.1007/s00339-018-1782-3.

Oganesvan, G., Galstyan, A., Mnatsakanyan, V., et al, 1991. Phenolic and flavonoid compounds of Ziziphora clinopodioides. Chem Nat 27, 247. https://doi.org/10.1007/BF00629776.

Arulmozhi, V., Pandian, K., Mirunalini, S., 2013. Ellagic acid encapsulated chitosan nanoparticles for drug delivery system in

human oral cancer cell line (KB). Colloids Surf. B Biointerfaces 110, 313–320. https://doi.org/10.1016/j.colsurfb.2013.03.039.

You, C., Han, C., Wang, X., et al, 2012. The progress of silver nanoparticles in the antibacterial mechanism, clinical application and cytotoxicity. Mol. Biol. Rep. 39, 9193–9201. https://doi.org/10.1007/s11033-012-1792-8.

Radini, I.A., Hasan, N., Malik, M.A., et al, 2018. Biosynthesis of iron nanoparticles using Trigonella foenum-graecum seed extract for photocatalytic methyl orange dye degradation and antibacterial applications. J. Photochem. Photobiol., B 183, 154–163. https://doi.org/10.1016/j.jphotobiol.2018.04.014.

Sankar, R., Maheswari, R., Karthik, S., et al, 2014. Anticancer activity of Ficus religiosa engineered copper oxide nanoparticles. Mat Sci Eng C 44, 234–239.

Sangami, S., Manu, M., 2017. Synthesis of Green Iron Nanoparticles using Laterite and their application as a Fenton-like catalyst for the degradation of herbicide Ametryn in water. Environ. Technol. Innov. 8, 150–163. https://doi.org/10.1016/j.eti.2017.06.003.

Katata-Seru, L., Moremedi, T., Aremu, O.S., et al, 2018. Green synthesis of iron nanoparticles using Moringa oleifera extracts and their applications: Removal of nitrate from water and antibacterial activity against Escherichia coli. J. Mol. Liq. 256, 296–304. https://doi.org/10.1016/j.molliq.2017.11.093.